

# Photocatalytic Degradation of Malachite Green and Rhodamine-B Using Titanium dioxide and Silver Nanoparticles: A Comparative Study

Sheeba Daniel and T. Ajitha

Department of Chemistry, Holy Cross College (Autonomous), Nagercoil, Tamil Nadu, India

## ABSTRACT

*The present investigation focuses on the photocatalytic activity of titanium dioxide and silver nanoparticles (AgNPs) on the degradation of malachite green and rhodamine-B dyes. Silver nanoparticles are synthesized using Emblica officinalis (gooseberry) extract. The synthesized AgNPs are characterized by UV-Visible and FT-IR spectroscopy. The nature and the particle size of AgNPs are determined using XRD analysis. The photocatalytic activity of the TiO<sub>2</sub> and AgNPs are examined on malachite green and rhodamine-B dyes under visible light illumination. The rate of photodegradation and degradation efficiency of malachite green using TiO<sub>2</sub> nanoparticles are  $7.04 \times 10^{-3} \text{ sec}^{-1}$  and 50 %. The rate of photodegradation and degradation efficiency of malachite green using AgNPs are  $1.18 \times 10^{-2} \text{ sec}^{-1}$  and 69.23 %. Malachite green undergoes photodegradation in the presence of TiO<sub>2</sub> and AgNPs and it acts as a catalyst for the degradation of malachite green. Rhodamine-B does not undergo photodegradation in the presence of TiO<sub>2</sub> and AgNPs. The absorption kinetics of the dye follows the pseudo-first order mechanism. Thus, the photodegradation proposed in this study may shed some light on future applications for the decolouration of dyes.*

**Keywords:** Malachite green; Rhodamine-B; Photocatalytic degradation; Degradation efficiency.

## 1. Introduction

Dyes are synthetic organic compounds having complex aromatic molecular structures and are difficult to biodegrade [1]. The removal of non-biodegradable dyes from the environment is a crucial ecological problem and many techniques are used for fading dyes [2]. Various physical techniques such as adsorption on activated carbon, ultra-filtration, reverse osmosis, coagulation by chemical agents, ion exchange on synthetic adsorbent resins, etc., have been used for the removal of dye pollutants. Advanced oxidation processes such as Fenton and Photo-Fenton catalytic reactions [3], H<sub>2</sub>O<sub>2</sub>/UV processes [4] have also been used for the removal of dyes from wastewater. Photocatalysis is a kind of advanced oxidation process recently used for the degradation of organic pollutants. Photocatalytic degradation has a great potential to control aqueous contaminants or pollutants. The photocatalysts used for photodegradation are able to photosensitize the complete mineralization of a wide range of compounds, like dyes, phenols, and pharmaceutical drugs, without producing harmful by-products at room temperature and pressure [5].

Malachite green is a triphenylmethane dye used in the textile and fish farming industries as a biocide [6]. It is an unsafe dye which possesses toxic properties affecting the cells of mammals and cause tumour in liver. This dye discharged in water bodies, hampers the life-cycle of aquatic animals and plants by obstructing the penetration of sunlight [7]. Scientific evidence indicated that malachite green dye and its reduced form leucomalachite green, might persist in edible fish tissues for extended periods of time [8]. Due to this significant health risks to human and fish, it is essential to remove malachite green from water or industrial effluent. Rhodamine-Bis a xanthene dye is used in

the textile industry, it is carcinogenic and toxic, inhalation and ingestion may cause liver and thyroid damage [9]. So effective treatment methods need to be implied for the degradation of rhodamine-B dye in wastewater.

Recently, metal nanoparticles act as effective photocatalysts for the degrading of dyes at room temperature with visible light illumination [10]. Many semiconductors have been synthesized and studied as photocatalysts of these,  $\text{TiO}_2$  has been found to be the most suitable one for environmental remediation [11]. Tanaka *et al.* [12] reported that catalytic activity of the anatase is much higher than the catalytic activity of the rutile. Besides the crystalline structure the catalytic activity of  $\text{TiO}_2$  can be also influenced by its particle size.

Green synthesis of nanoparticles is an emerging branch of nanotechnology. The synthesis of nanomaterials is of current interest due to their wide variety of applications in the fields of electronics, photonics, catalysis, medicine, etc. Biosynthesis of nanoparticles provides advancement over chemical and physical methods as it is cost effective and eco-friendly. Recently biosynthesised silver nanoparticles (AgNPs) are also used as photocatalyst for the degradation of dyes [13]. Green synthesised AgNPs are commonly utilized nanomaterials due to specific surface area and is relevant for catalytic reactivity, high electrical conductivity and unique optical properties that could be used in various applications. Based on the literature survey, the present study focuses on the photocatalytic degradation of malachite green and rhodamine-B using  $\text{TiO}_2$  nanoparticles and AgNPs. The present investigation is carried out to identify the photocatalytic activity of  $\text{TiO}_2$  nanoparticles and AgNPs on malachite green and rhodamine-B dyes. The green synthesised AgNPs from *Emblica officinalis* (gooseberry) extract is characterized by UV-Visible spectroscopy and FT-IR spectroscopy. The nature and the particle size of AgNPs is determined by XRD analysis.

## **2. Experimental Session**

### **2.1 Materials**

Fresh and ripened gooseberry was obtained from the local market. Silver nitrate, malachite green and rhodamine-B were procured from Merck. Titanium dioxide nanopowder of particle size less than 25 nm was purchased from Sigma-Aldrich. Double distilled deionised water was used as a solvent for the synthesis as well as for the degradation studies.

### **2.2 Synthesis of AgNPs from gooseberry extract**

1 mM aqueous solution of  $\text{AgNO}_3$  was prepared and used for the synthesis of silver nanoparticles. 10 mL of gooseberry extract was added to 90 mL of 1 mM aqueous  $\text{AgNO}_3$  solution in a 250 mL Erlenmeyer flask and incubated at room temperature. The sample colour changes from colourless to light grey colour within 10 minutes indicate the formation of AgNPs. The AgNPs obtained by gooseberry extract was centrifuged at 15,000 rpm for 5 min and subsequently dispersed

in sterile distilled water to get rid of any uncoordinated biological materials. The pellet of AgNPs collected at the bottom of the centrifuge tube was collected, dried and stored at  $-4^{\circ}\text{C}$ .

### 2.3 Instrumentation Techniques

The absorption spectrum of AgNPs and the photodegradation of dye were carried out using Shimadzu UV-1800 spectrophotometer. FT-IR analysis of the dried AgNPs was carried out through the potassium bromide (KBr) pellet (FT-IR grade) method in 1:100 ratio and the spectrum was recorded using Shimadzu IR Affinity-1 FT-IR spectrophotometer with the range of  $4000\text{-}400\text{ cm}^{-1}$  at the resolution of  $4\text{ cm}^{-1}$ . Phase formation of the synthesized nanoparticles was characterized by X-ray diffraction. Diffraction data for the nanoparticles on glass slides were recorded on an X-ray diffractometer (Ultima III, Rigaku, Tokyo, Japan) with Cu  $K\alpha$  radiation ( $\lambda = 1.5406\text{ \AA}$ ) source in the  $2\theta$  range of  $10^{\circ}\text{-}80^{\circ}$  with  $4^{\circ}/\text{minute}$  scanning rate. The particle size was calculated from the width of the XRD peaks using the Scherrer formula.

$$D = 0.94 \lambda / \beta \cos \theta$$

where  $D$  is the average crystallite domain size perpendicular to the reflecting planes,  $\lambda$  is the X-ray wavelength,  $\beta$  is the full width at half maximum (FWHM) and  $\theta$  is the diffraction angle.

### 2.4 Photocatalytic degradation

The stock solution of  $1.0 \times 10^{-3}\text{ M}$  concentration of malachite green and rhodamine-B were prepared by dissolving the corresponding dyes in 100 mL of double distilled water. This stock solution was further diluted for degradation studies. The degradation of malachite green and rhodamine-B were studied separately by taking 100 mL of  $5.0 \times 10^{-5}\text{ M}$  of the dyes with and without catalyst in the presence of sunlight. The pH was maintained at 7.5, an aliquot of 4.0 mL was taken out from the reaction mixtures at regular time intervals and the absorbance was measured at 620 nm for malachite green and 540 nm for rhodamine-B. The progress of the photocatalytic reaction was observed by measuring the absorbance at regular time intervals. The decrease in absorbance with increasing time intervals shows the degradation of dye. The degradation efficiency ( $\eta$ ) was described by the equation:

$$\eta = (A_0 - A)/A_0 \times 100\%$$

Where  $A_0$  and  $A$  was the absorption intensities at the beginning and after photocatalytic reaction for certain time.

## 3. Results and Discussion

The characterization of the silver nanoparticles and the detailed study on the catalytic degradation of malachite green and rhodamine-B dye with  $\text{TiO}_2$  nanoparticles and AgNPs in the presence of sunlight are reported in this section.

### 3.1 Absorption spectral analysis of AgNPs

Reduction of silver ion into AgNPs during exposure to the gooseberry extract could be followed by colour change. Silver nanoparticles exhibits light grey colour in aqueous solution due to the surface plasmon resonance phenomenon, which results from collective oscillations of their conduction band electrons in response to electromagnetic waves. Absorption spectrum of AgNPs formed in the reaction media after 10 minutes has absorbance peak at 435 nm, broadening of peak indicated that the particles are polydispersed (**Fig. 1**). Similar results are also obtained for the green synthesis of AgNPs from *Euphorbia hirta L* and *Cissus Quadrangularis*[14].

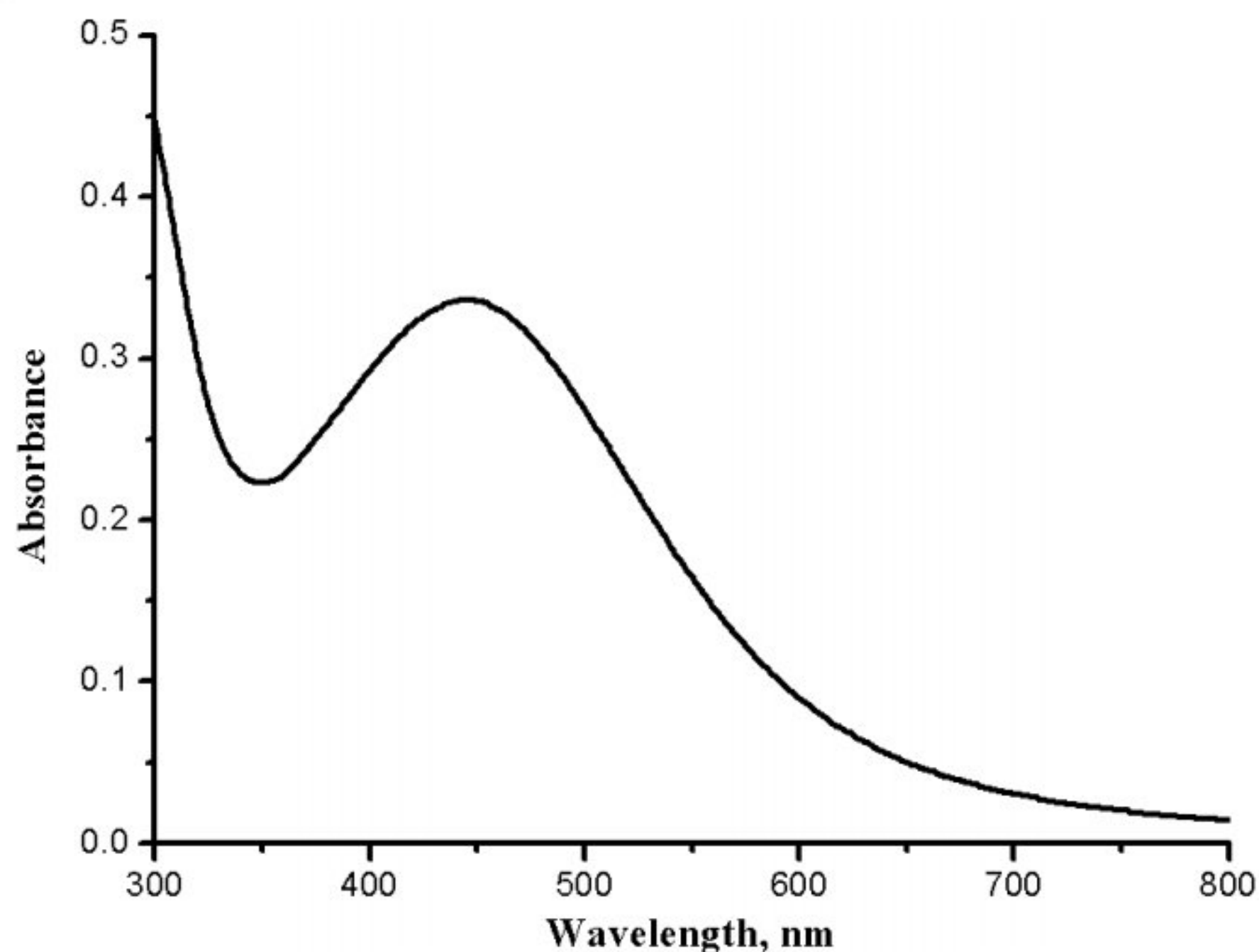


**Fig. 1** Absorption spectrum of AgNPs synthesized from gooseberry extract

### 3.2 FTIR analysis of AgNPs

FT-IR measurement is carried out to identify the biomolecules which can act as capping and stabilizing agent for the synthesis of AgNPs. The FT-IR spectrum of the synthesized AgNPs(**Fig. 2**) shows absorption bands at 3424, 2918, 2864, 1691, 1651, 1582, 1535, 1457, 1022, 906 and 680  $\text{cm}^{-1}$ . The prominent band around 3424  $\text{cm}^{-1}$  signified the O-H stretching of alcohols. The presence of weak band at 2918 and 2864  $\text{cm}^{-1}$  corresponds to the C-H stretching of alkane. Absorption band at 1691  $\text{cm}^{-1}$  is due to C=O stretching modes of esters present in ascorbic acid. IR spectrum exhibits weak bands at 1651, 1582 and 1457  $\text{cm}^{-1}$  are due to the stretching vibration of C=C bond. The weak band at 1022  $\text{cm}^{-1}$  is assigned for the C-O stretching of primary alcohols. C-H bending vibrations occur at 906 and 680  $\text{cm}^{-1}$  respectively. FT-IR spectrum confirms that the ascorbic acid present in the gooseberry extract can act as the capping and stabilizing agent, which reduce the  $\text{Ag}^+$  ions to  $\text{Ag}^0$  and stabilize the AgNPs. The mechanism of the reduction of  $\text{Ag}^+$  ions to  $\text{Ag}^0$  may be due to the presence of water-soluble antioxidant substances like ascorbic acid which is present in the

gooseberry extract. Ascorbic acid is the reducing agent and can reduce and thereby neutralize, reactive oxygen species leading to the formation of ascorbate radical and an electron. This free electron reduces the  $\text{Ag}^+$  ions to  $\text{Ag}^0$  (Scheme 1).

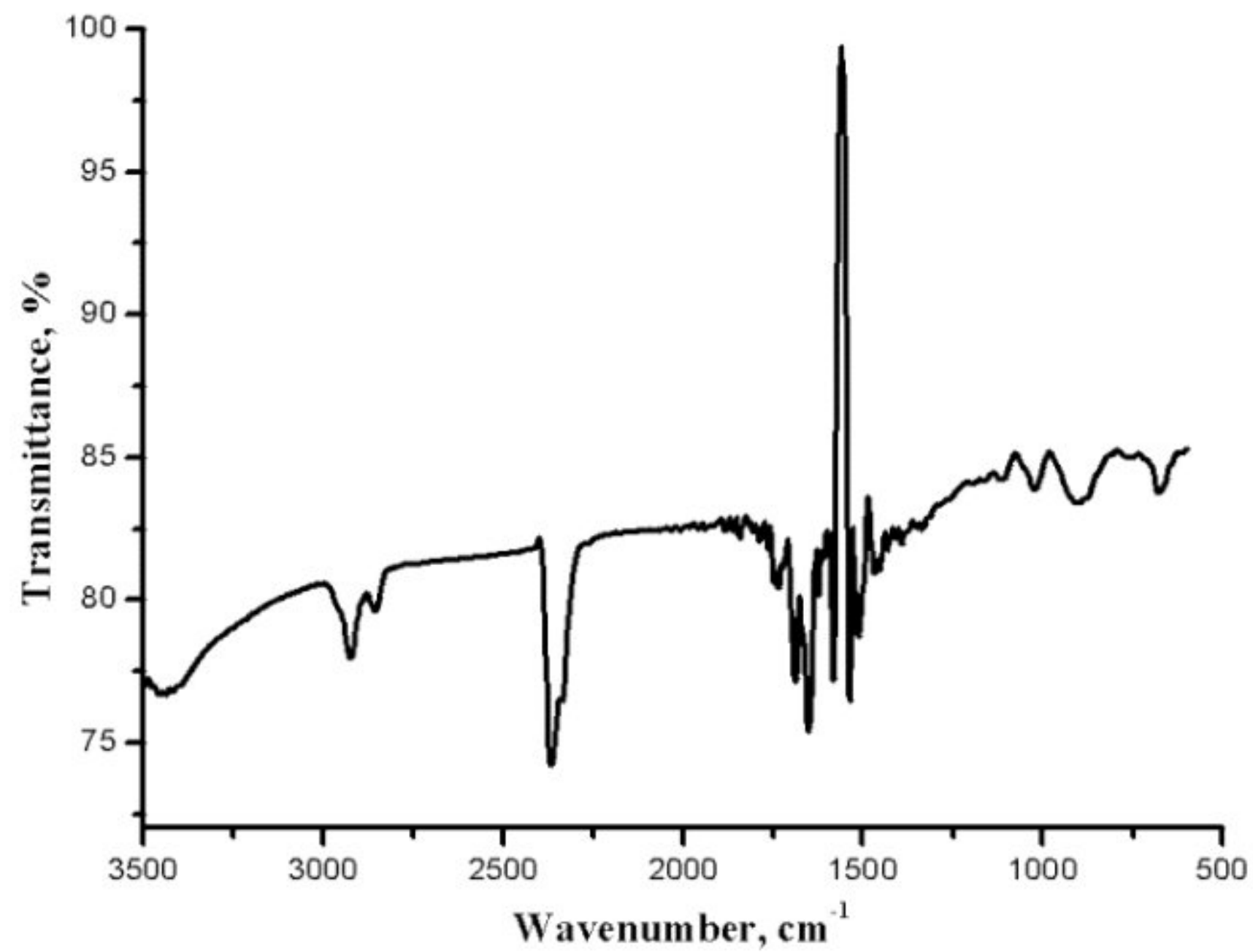
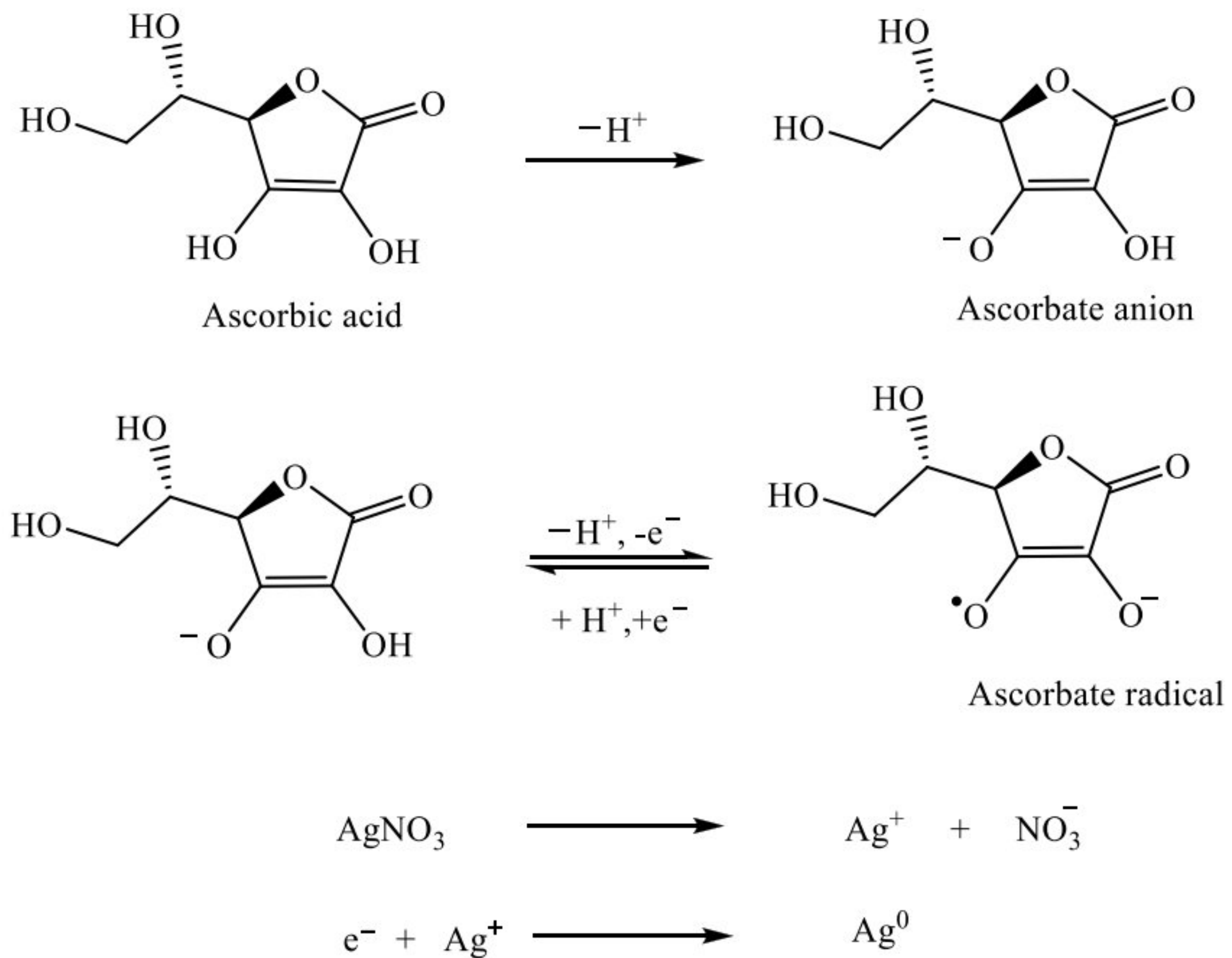


**Fig. 2** FT-IR spectrum of AgNP synthesized from gooseberry extract



**Scheme 1** Ascorbic acid reduction of  $\text{Ag}^+$  to  $\text{Ag}^0$

### 3.3 XRD analysis

X-ray diffraction (XRD) analysis is carried out for  $\text{TiO}_2$  and synthesised AgNPs, nanoparticles. The crystalline size can be determined by Scherrer formula. The diffractogram of AgNPs (**Fig. 3**) has been compared with the standard powder diffraction card of JCPDS, silver file No. 65-2871. Four peaks at  $2\theta$  values of 37.947, 44.219, 64.240 and 77.257 degree in the experimental diffractogram have been identified due to silver metal and the corresponding (hkl) values are (111), (200), (220) and (311). The crystalline size of AgNPs obtained from the FWHM peak at 37.947 is 25 nm. The XRD study thus confirmed face centered cubic geometry for the AgNPs.

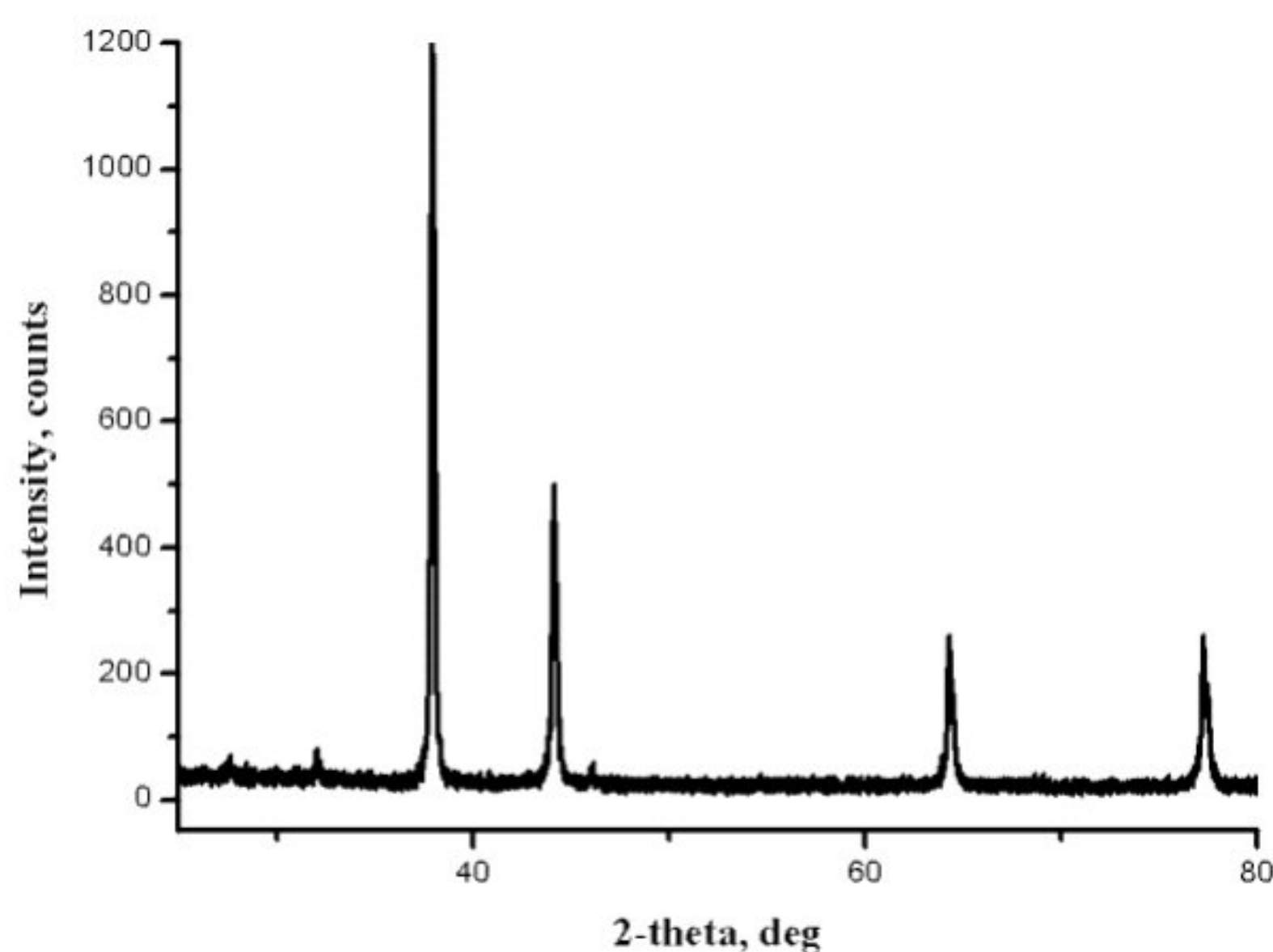


**Fig. 3** XRD pattern of AgNPs synthesized from gooseberry extract

The diffractogram of  $\text{TiO}_2$  nanoparticles (**Fig. 4**) has been compared with the standard powder diffraction card of JCPDS,  $\text{TiO}_2$  file No. 89-4921. Nine peaks at  $2\theta$  values of 25.181, 37.468, 47.942, 53.856, 54.918, 62.519, 68.579, 70.265 and 75.117 degree in the experimental diffractogram have been identified due to  $\text{TiO}_2$  and the corresponding (hkl) values are (101), (103), (200), (105), (211), (213), (116), (220) and (215). The crystalline size of  $\text{TiO}_2$  obtained from the FWHM peak at 25.181 is 24 nm. The XRD study confirmed body centered tetragonal geometry for  $\text{TiO}_2$  nanoparticles.

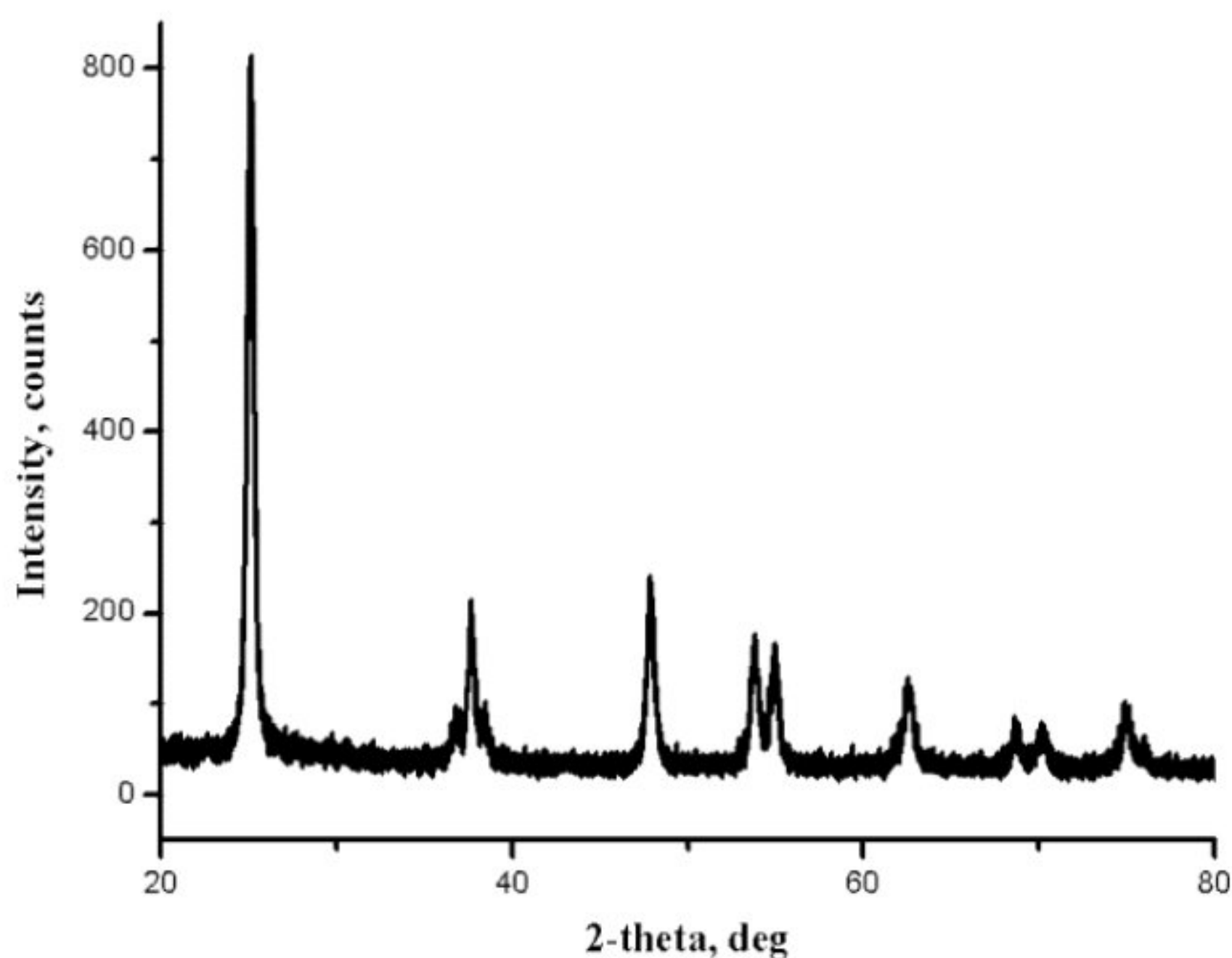


**Fig. 4** XRD pattern of TiO<sub>2</sub> nanoparticles

### 3.4 Photodegradation of malachite green

The change in absorbance of malachite green at 620 nm with and without TiO<sub>2</sub> nanoparticles and AgNPs are reported in the **Tables 1 - 3**. The results revealed that the absorbance of the solution decreases with increasing time intervals showing thereby that the concentration of the dyes decreases with increasing time of exposure. A plot of  $1 + \log A$  versus time is linear and follows pseudo-first order kinetics (**Figs.5 - 7**), where A is the absorbance of the medium at a particular time t. The rate constant is measured by following expression:

$$k = - 2.302 \times \text{slope}$$

**Table 1** Photodegradation of malachite green without catalyst at various time intervals

Time (min)	Absorbance (A)	1 + log A
0.0	0.52	0.7160
10	0.51	0.7076
20	0.49	0.6901
30	0.47	0.6721
40	0.43	0.6334
50	0.42	0.6232
60	0.41	0.6127
70	0.38	0.5797
80	0.37	0.5682
90	0.35	0.5440
100	0.34	0.5314

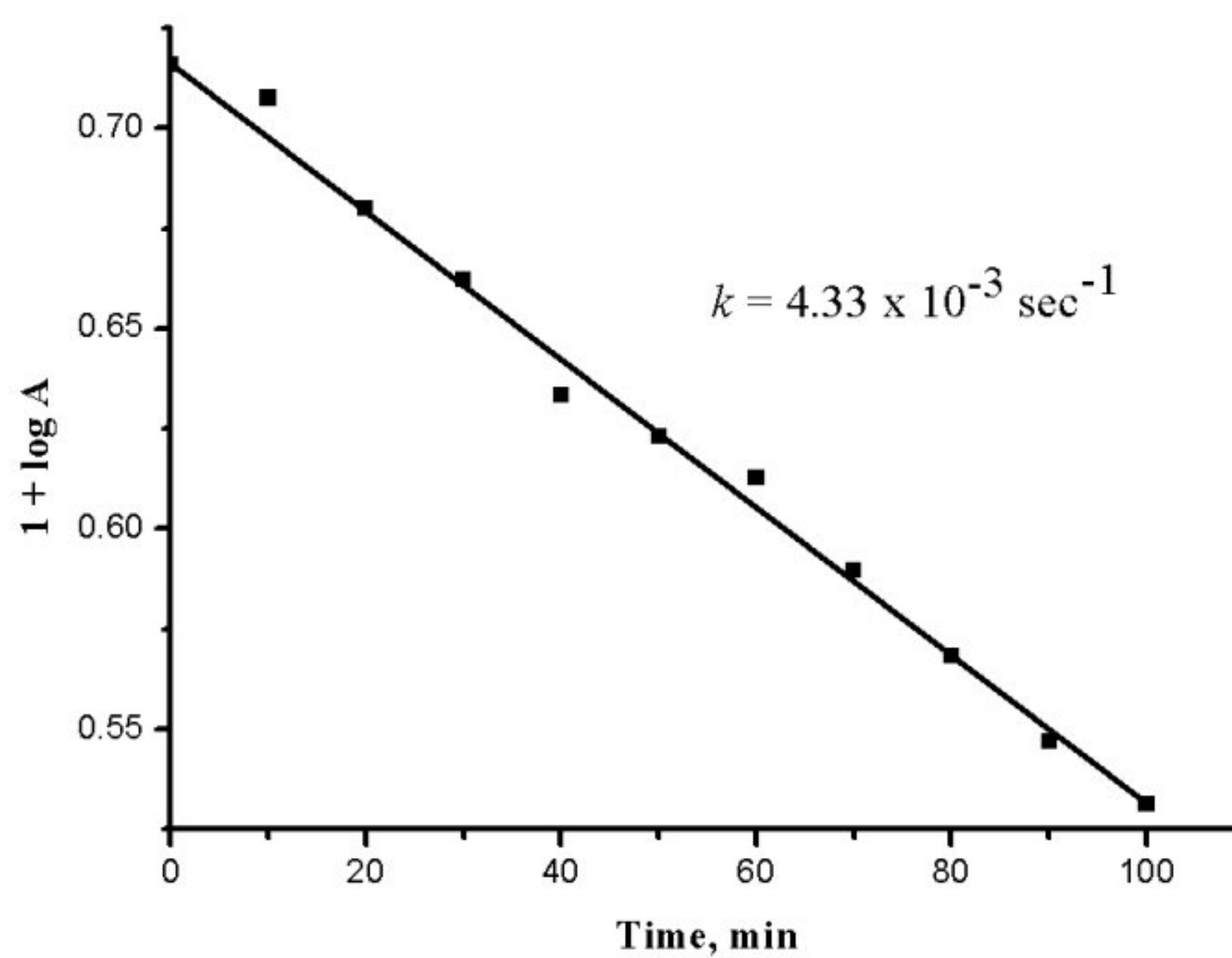


**Fig. 5** Plot of  $1 + \log A$  vs time for malachite green without catalyst

**Table 2** Photodegradation of malachite green with 0.01 g of  $\text{TiO}_2$  nanoparticles at various time intervals

Time (min)	Absorbance (A)	$1 + \log A$
0.0	0.52	0.7160
10	0.49	0.6901
20	0.46	0.6627
30	0.45	0.6532
40	0.43	0.6334
50	0.39	0.5910
60	0.37	0.5682
70	0.32	0.5051
80	0.30	0.4771
90	0.28	0.4471
100	0.26	0.4149



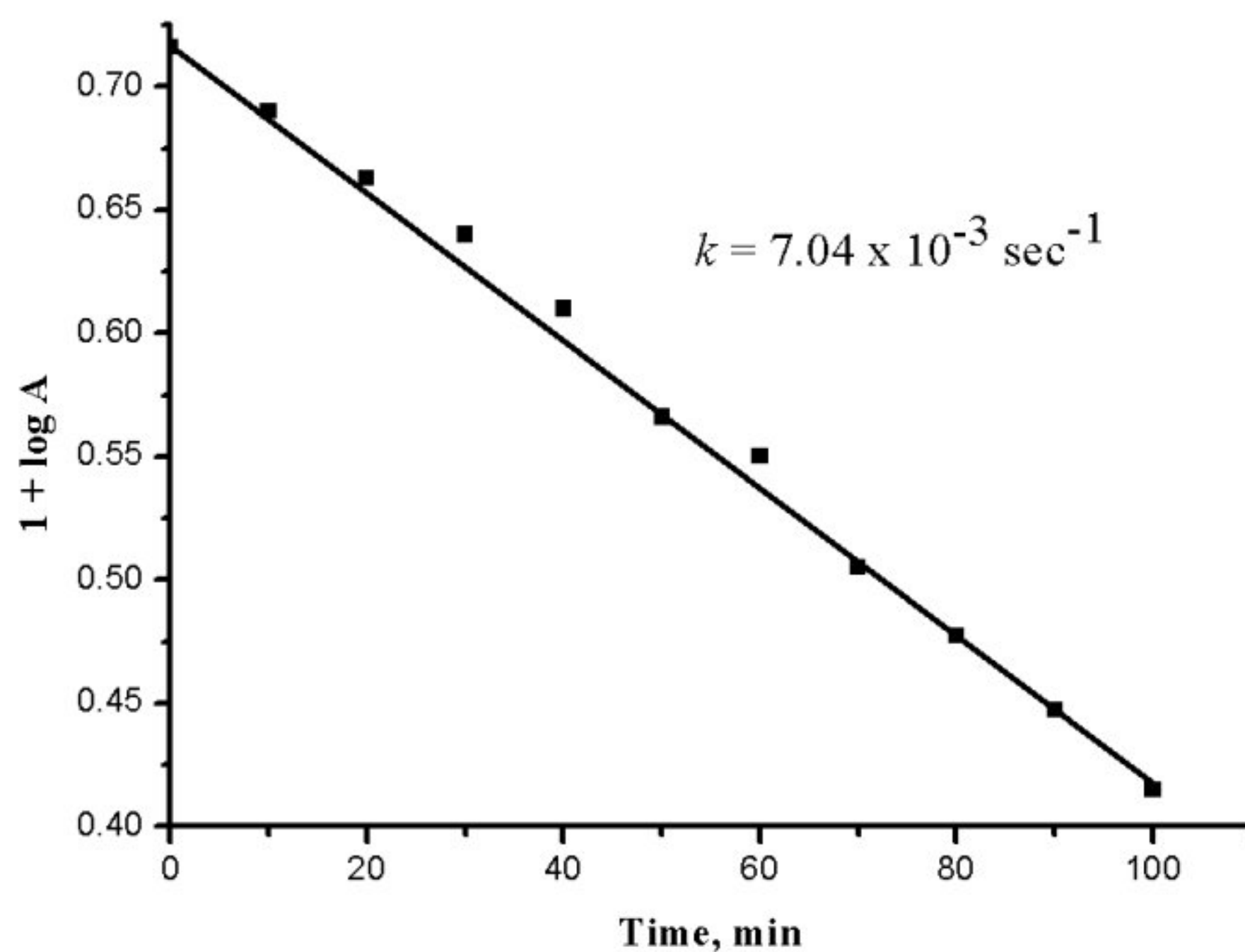


**Figure 6** Plot of  $1 + \log A$  vs time for malachite green with 0.01 g of  $\text{TiO}_2$  nanoparticles

**Table 3** Photodegradation of malachite green with 0.01 g of AgNPs at various time intervals

Time (min)	Absorbance (A)	$1 + \log A$
0.0	0.52	0.7160
10	0.45	0.6532
20	0.40	0.6020
30	0.36	0.5563
40	0.33	0.5185
50	0.30	0.4771
60	0.28	0.4471
70	0.22	0.3424
80	0.18	0.2552
90	0.17	0.2304
100	0.16	0.2041

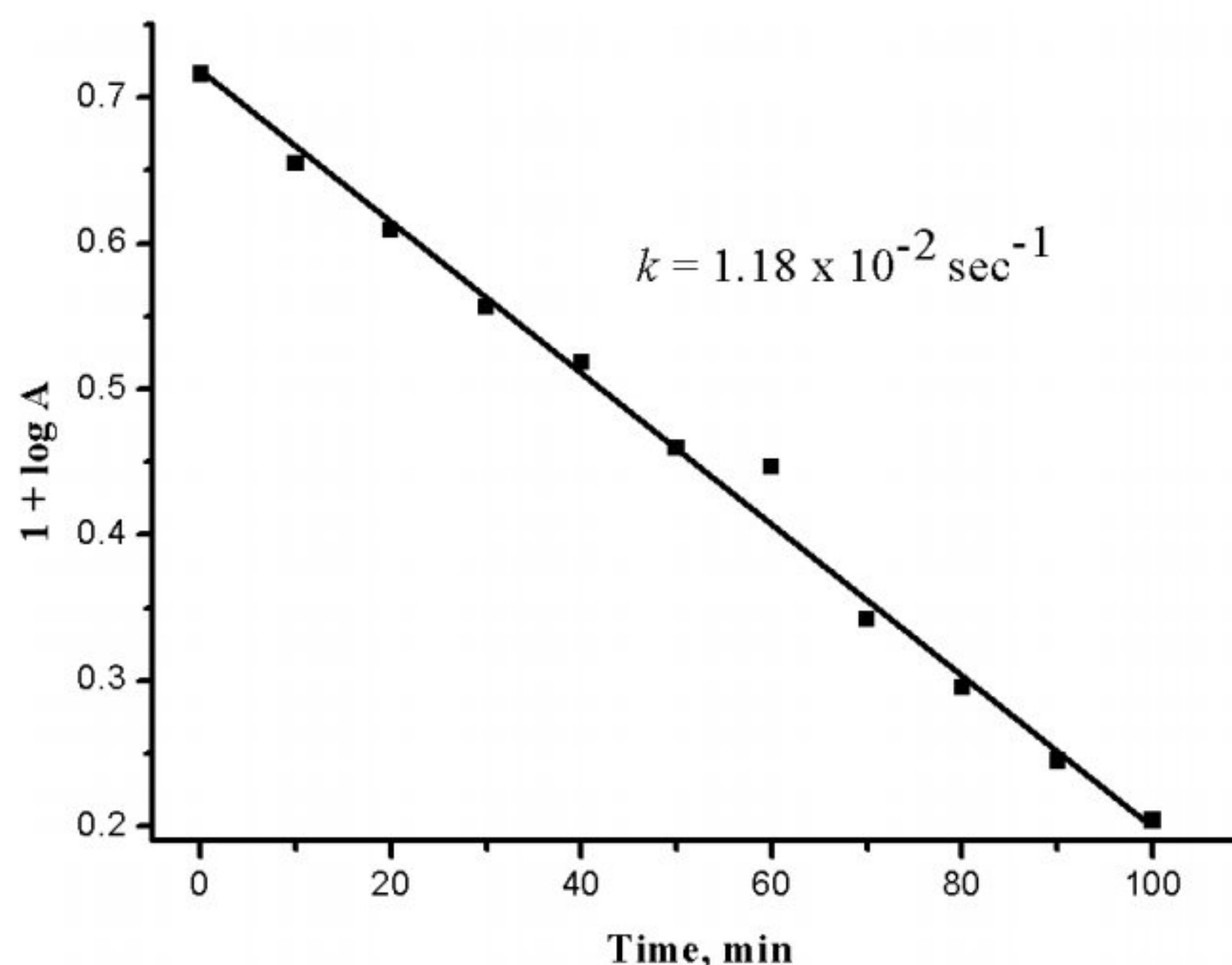
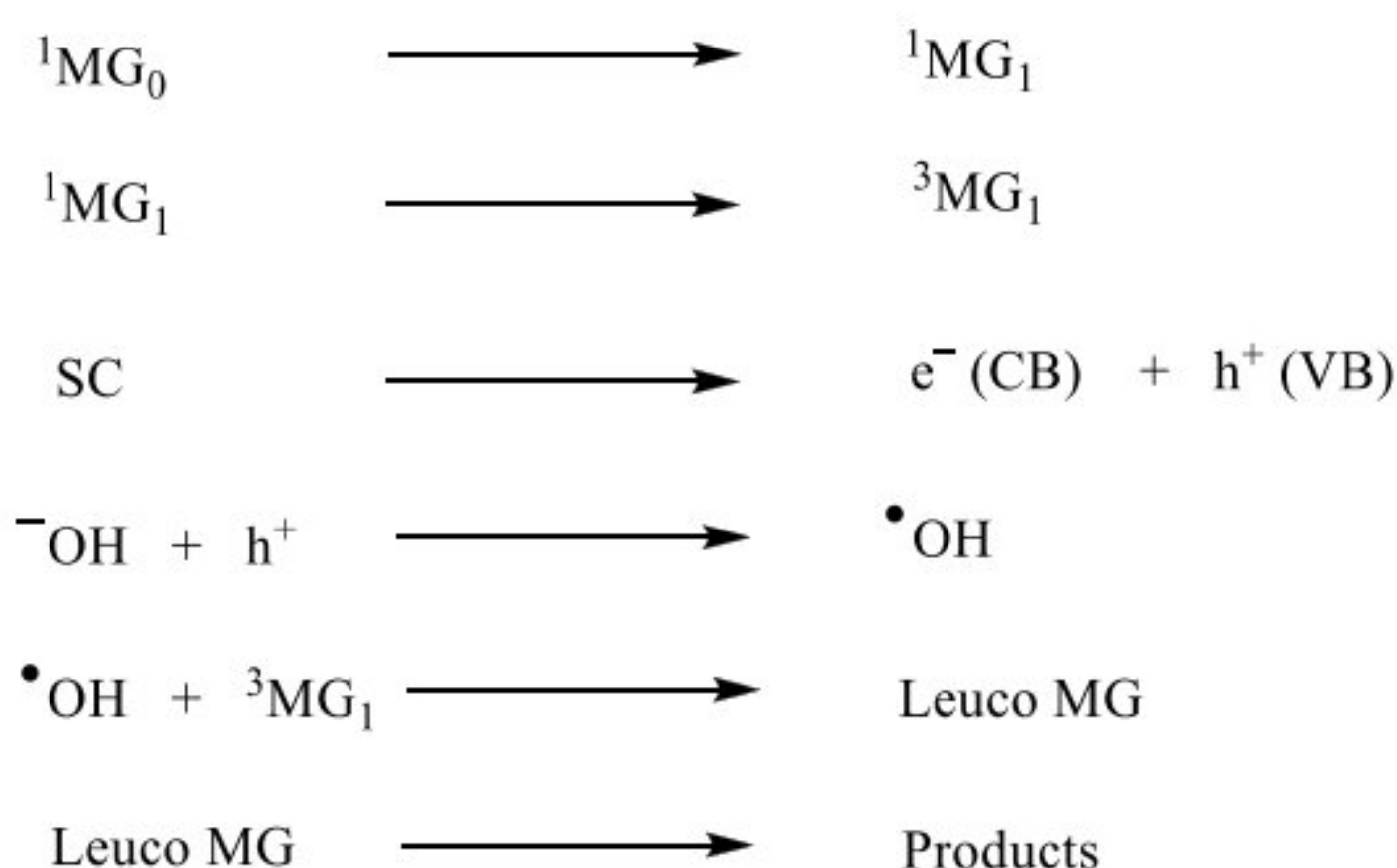


**Fig. 7** Plot of  $1 + \log A$  vs time for malachite green with 0.01 g of AgNPs

The rate of photodegradation and degradation efficiency of malachite green without catalyst are  $4.33 \times 10^{-3} \text{ sec}^{-1}$  and 34.61 %. The rate of photodegradation and degradation efficiency of malachite green using 0.01 g of  $\text{TiO}_2$  nanoparticles are  $7.04 \times 10^{-3} \text{ sec}^{-1}$  and 50 %. The rate of photodegradation and degradation efficiency of malachite green using 0.01 g of AgNPs are  $1.18 \times 10^{-2} \text{ sec}^{-1}$  and 69.23 %. The degradation efficiency of malachite green with AgNPs is higher than that of  $\text{TiO}_2$  nanoparticles. Thus, the AgNPs synthesised from gooseberry extract acts as an efficient photocatalyst for the degradation of malachite green. On the basis of these observations, a tentative mechanism for photocatalytic degradation of malachite green is proposed as follows:



Malachite green (MG) absorbs radiations of suitable wavelength and gives rise to its first excited singlet state. Then it undergoes intersystem crossing (ISC) to give the triplet state of

the dye. On the other hand, the semiconducting nanoparticles of titanium dioxide and silver (SC) also utilize the radiant energy to excite its electron from valence band to the conduction band. An electron can be abstracted from hydroxyl ion by the hole ( $h^+$ ) present in the valence band of semiconductor generation OH radical. This hydroxyl radical oxidize malachite green to its leuco form, which may ultimately degrade to products.

### 3.5 Photodegradation of Rhodamine-B

The change in absorbance of rhodamine-B with and without  $TiO_2$  nanoparticles and AgNPs are determined at 540 nm and are reported in the **Tables 4 - 6**. The absorbance of rhodamine-B with catalyst is noted at regular time intervals, the absorbance of the solution first decreases and then increases with increasing time intervals.

**Table 4** Photodegradation of rhodamine-B without catalyst at various time intervals

Time (min)	Absorbance (A)
0.0	0.45
10	0.45
20	0.45
30	0.44
40	0.44
50	0.44
60	0.43
70	0.41
80	0.40
90	0.40
100	0.40

**Table 5** Photodegradation of rhodamine-B with 0.01 g of  $TiO_2$  nanoparticles at various time intervals

Time (min)	Absorbance (A)
0.0	0.45
10	0.43
20	0.41
30	0.41
40	0.42
50	0.44
60	0.44
70	0.45
80	0.47
90	0.49
100	0.53

**Table 6** Photodegradation of rhodamine-B with 0.01 g of AgNPs at various time intervals

Time (min)	Absorbance (A)
0.0	0.45
10	0.42
20	0.40
30	0.39
40	0.38
50	0.39
60	0.39
70	0.41
80	0.43
90	0.45
100	0.49

These results thereby indicate that the concentration of rhodamine-B dye increases with increasing time of exposure. The increase in concentration of rhodamine-B dye indicates that it does not degrade by TiO<sub>2</sub> nanoparticles and AgNPs. Therefore, rhodamine-B does not undergo photodegradation in the presence of TiO<sub>2</sub> nanoparticles and AgNPs. Hence TiO<sub>2</sub> nanoparticles and AgNPs are not a suitable catalyst for the degradation of rhodamine-B. Thus in the present investigation TiO<sub>2</sub> nanoparticles and AgNPs act as a catalyst only for the degradation of malachite green not for rhodamine-B.

### Conclusion

The present investigation deals about the feasibility of TiO<sub>2</sub> nanoparticles and AgNPs for the removal of malachite green and rhodamine-B dyes from aqueous solution. The green synthesised AgNPs from gooseberry extract are characterized by UV-Visible and FT-IR spectral analysis. The FTIR spectrum confirms the involvement of ascorbic acid in the reduction and stabilization of the AgNPs. The particle size of synthesised AgNPs and TiO<sub>2</sub> nanoparticles obtained from XRD analysis are 25 and 24 nm. The rate of photodegradation and degradation efficiency of malachite green using TiO<sub>2</sub> nanoparticles (0.01 g) are  $7.04 \times 10^{-3} \text{ sec}^{-1}$  and 50 %. The rate of photodegradation and degradation efficiency of malachite green using AgNPs (0.01 g) are  $1.18 \times 10^{-2} \text{ sec}^{-1}$  and 69.23 %. Rhodamine-B does not undergo photodegradation in the presence of TiO<sub>2</sub> nanoparticles and AgNPs. The absorption kinetics of the dye follows the pseudo-first order mechanism. The result reveals that AgNPs act as a catalyst for the removal of malachite green. Thus, the photodegradation proposed in this study may shed some light on future applications for the decolouration of dyes.

## References

1. Daneshvar, N., Ayazloo, M., Khataee, A.R., Pourhassan, M., Biological decolorization of dye solution containing Malachite Green by microalgae *Cosmarium* sp, *Bioresource Technology*, 98 (2007) 1176 - 1182.
2. Kumar, A., Choudhary, P., Verma, P., A comparative study on the treatment methods of textile dye effluents, *Global J. Environ. Res.*, 5 (2011) 46 - 52.
3. Prado, A.G.S., Bolzon, L.B., Pederso, C.P., Moura, A.O., Costa, L.L., Nb<sub>2</sub>O<sub>5</sub> as efficient and recyclable photocatalyst for Indigo Carmine degradation, *Appl. Catal. B: Environ.*, 82 (2008) 219 - 224.
4. Hossain, M.A., Hassan, M.T., Kinetic and thermodynamic studies of the adsorption of crystal violet onto used black tea leaves, *Orbital Elec. J. Chem.*, 5 (2013) 150 - 156.
5. Kansal, S.K., Hassan, A., Ali, A., Kappor, S., Photocatalytic decolorization of biebrich scarlet dye in aqueous phase using different nanophotocatalysts, *Desalination*, 259 (2010) 147-155.
6. Chen, C.Y., Kuo, Y.T., Cheng, C.Y., Huang, Y.T., Ho, I.H., Chung, Y.C., Biological decolorization of dye solution containing malachite green by *Pandoraepulmonicola* YC32 using a batch and continuous system, *Journal of Hazardous Materials*, 172 (2009) 1439-1445.
7. Gupta, V.K., Suhas, A., Application of low-cost adsorbents for dye removal - A review, *Journal of Environmental Management*, 90 (2009) 2313 - 2342.
8. Sudova, E., Machova, J., Svobodova, Z., Vesely, T., Negative effects of malachite green and possibilities of its replacement in the treatment of fish eggs and fish: a review, *VeterinariMedicina*, 52 (2007) 527 - 539.
9. Mittal, A., Malviya, A., Kaur, D. Mittal, J., Kurup, L., Studies on the adsorption kinetics and isotherms for the removal and recovery of Methyl Orange from wastewaters using waste materials, *Journal of Hazardous Materials*, 148 (2007) 229 - 240.
10. Talib, T.H., AlDamen, M.A., Alani, R.R., Modeling of advanced photooxidation of Alizarin Red-S dye using TiO<sub>2</sub> as photocatalyst, *American Chemical Science Journal*, 4, (2014) 918 - 933.
11. Tayade, R.J., Suroliya, P.K, Kularani R.G, Jasra R.V., Photocatalytic degradation of dyes and organic contaminants in water using nanocrystalline anatase and rutile TiO<sub>2</sub>, *Sci. Technol. Adv. Mater.*, 8 (2007) 455 - 462.
12. Tanaka, K., Lapule, M.F.V., Hisanaga, T., Effect of crystallinity of TiO<sub>2</sub> on its photocatalytic action, *Chemical Physics Letters*, 187 (1991) 373 - 379.
13. Jegadeeswaran, P., Rajiv, P., Shivaraj, R., Venckatesh, R., Photocatalytic degradation of dye using brown seaweed (*Padinatetrastromatica*) mediated silver nanoparticles, *J. Bio Sci. Res.*, 3 (2012) 229 - 233.
14. Elumalai, E.K., Prasad, T.N.V.K.V., Kambala, V., Nagajyothi, P.C., David, E., Green synthesis of silver nanoparticle using *Euphorbia hirta* L and their antifungal activities, *Archives of Applied Science Research*, 2 (2010) 76 - 81.